CHEMISTRY
A EUROPEAN JOURNAL

DOI: 10.1002/chem.200600511

Investigation of a Molecular Morphology Effect on Polyphenylazomethine Dendrimers; Physical Properties and Metal-Assembling Processes

Takane Imaoka, Reiko Tanaka, and Kimihisa Yamamoto*[a]

Abstract: A series of novel dendritic polyphenylazomethines (DPA) with asymmetric morphologies was synthesized. Their physical properties, such as encapsulating effect, molecular dynamics, and metal assembly, are strongly dependent on the entire conformation of the molecules. The most important property is layer-by-layer metal assembly in the dendrimer structure from the core to the outside. Bis- and tris-substituted DPAs of the fourth generation also act as frameworks for stepwise assembly of a metal component ($SnCl_2$), like the fully substituted symmetric DPA. However, extensive investigation of metal assembly in specific DPAs revealed that they do not follow the stepwise process. The molecular density calculated from the experimental hydrodynamic volume indicated that bis- and tris-substituted DPAs with asymmetric morphology still retain a free space similar to that of fully substituted symmetric DPA. The monosubstituted DPA, however, displayed a slightly higher density (smaller space) than the other DPAs. The experimental results suggest a bent conformation of the dendrimer in which the core moiety is folded into the dendron structure. In addition, the molecular dynamics were probed by means of the ^{1}H NMR signals of the porphyrin core. It was demonstrated that the conformation is not fixed at room temperature in solvated DPAs, especially in monosubstituted DPA. A similar observation was for the smaller DPAs (third generations) with asymmetric morphologies. These dendrimers do not follow the stepwise complexation process. The structures of bis- and tris-substituted dendrimers which accurately follow the stepwise process are fixed. These observations provide a new insight into the finely controlled metal-assembly chemistry of dendritic macromolecules, and a rigid and fixed conformation is one of important factors for their unique properties.

Keywords: dendrimers · molecular dynamics · N ligands · porphyrinoids · UV/Vis spectroscopy

Introduction

Metal-assembling macromolecular ligands of low polydispersity are key materials for size-controlled synthesis of metal nanoparticles in the solution phase.[1–3] Dendritic architecture is suitable for this concept because it may allow multiple metal ions to be bound.[4–8] The spherical topology and uniform molecular weight[9–15] would greatly contribute to templated nanoparticle synthesis. However, most dendrimer ligands, such as poly(amidoamine) (PAMAM), randomly assemble metal ions in spite of their unimolecular structure. In the metal-assembling process, electronic repulsion between the cationic metal ion and entropy relaxation should predominate. This would lead to a system with a polydisperse-metal-assembled structure in a monodisperse macromolecular ligand.[16]

Since the discovery of stepwise radial complexation in a dendritic polyphenylazomethine (DPA),[17] variations of this molecule were synthesized.[18–25] The DPA family of macromolecular ligands has a unique metal-assembling process in which metal ions bind to the branching monomer units in perfect order from the core to the outside termini. One of the principal driving forces for stepwise assembly may be a steep basicity gradient through the dendritic cascade structure, based on the strong electron-donating effect of the phenylazomethine building blocks stacked on the outer connections.[16]

In addition, it is likely that the rigid π-conjugated structure is indispensable for the unique metal-assembling property. Dendrimers with a flexible backbone tend to exhibit many conformations including backfolding of the terminal monomers into the core even at room temperature.[26–32]

[a] Dr. T. Imaoka, R. Tanaka, Prof. Dr. K. Yamamoto
Department of Chemistry, Keio University
223–8522 Yokohama (Japan)
Fax: (+81) 45-566-1718
E-mail: yamamoto@chem.keio.ac.jp

Supporting information for this article is available on the WWW under http://www.chemeurj.org/ or from the author.

Therefore, the exact position of each monomer unit in the flexible dendrimer cannot be defined. In contrast, the conformational variations of dendrimers composed of rigid backbones are far fewer, and backfolding is avoided.[33–35] Fine control of the coordination process is feasible for this type of dendrimer. The DPAs belong to the group of rigid dendrimers, as shown by their experimental hydrodynamic and solid-state properties.[19,24,36] A three-dimensional (3D) model obtained from MO calculations also indicates a stiff structure which prevents the folding of the termini. As a result, the DPA has enough space for full complexation of metal ions until every coordination site is filled.

It is important to elucidate how precise assembly is controlled in DPAs. The mechanism would help new molecular designs for advanced hybridized materials with macromolecular and metallic elements. Herein we report on metal coordination by zinc–porphyrin-cored DPAs in various molecular morphologies. Jiang and Aida reported that the number of dendrimer substituent at the porphyrin *meso* positions strongly affects their photo-energy-funneling properties through morphology-controlled molecular dynamics.[37] By the same token, the morphology should affect the coordination properties in dependence on the dynamics of the DPAs. The goal of this work was to determine the requirements for finely controlled metal assembly in dendritic macromolecules from the aspects of morphology and dynamics. The molecular form was investigated on the basis of the hydrodynamic parameters obtained from the intrinsic viscosity. The ^{1}H NMR signals predict the timescales of configurational changes in the dendrimer structure. These properties are related to $SnCl_2$ assembly, as was determined by titration with UV/Vis absorption spectroscopy.

Results

Synthesis and characterization of dendritic phenylazomethines (DPA) with different numbers of dendrons: Mono-, di-, and tridendronized zinc–porphyrins (Scheme 1: **ZnP-[D*n*]$_m$**, $n=1$–4, $m=1$–3) were prepared from zinc–*meso*-tetraphenylporphyrins with one, two, or three amino groups at the *para* positions of their *meso*-phenyl rings (**ZnP-[NH$_2$]$_m$**).

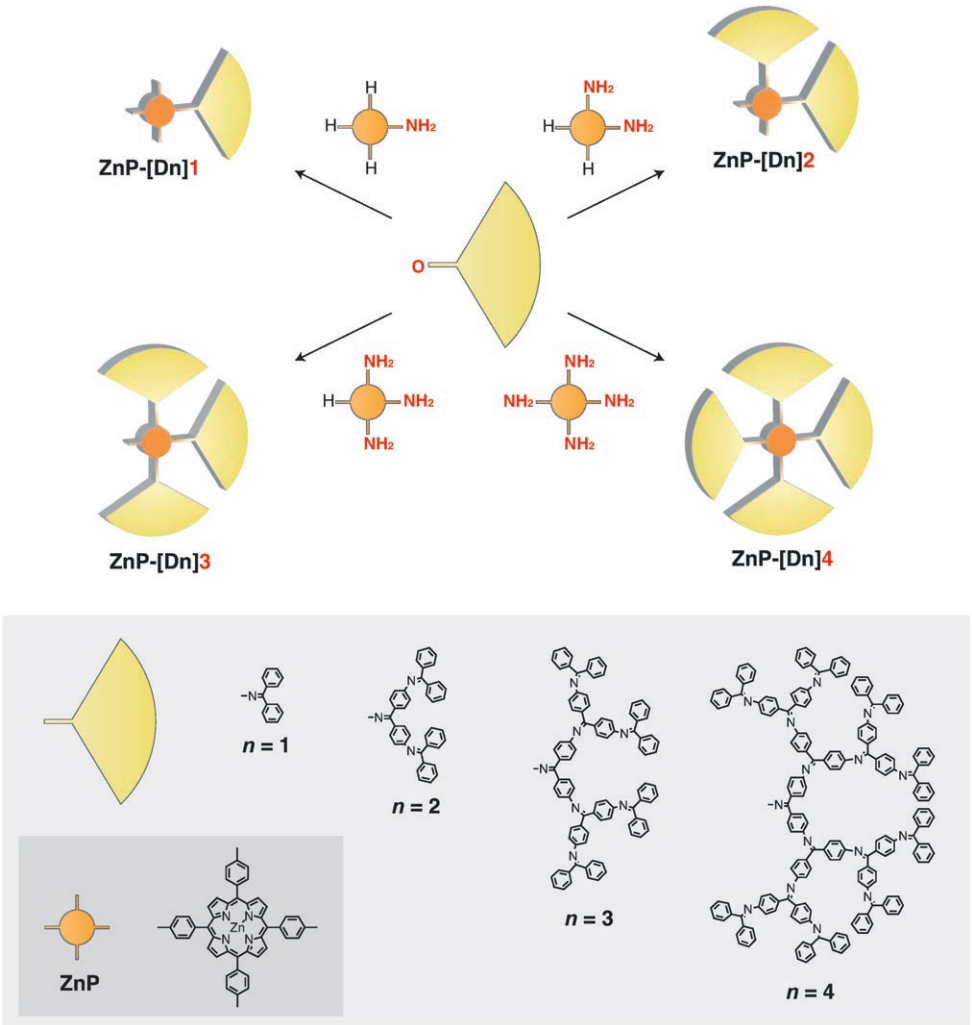

Scheme 1. Synthesis and structures of DPAs with a zinc–porphyrin core.

The aminoporphyrins were prepared by nitration of tetraphenylporphine (H_2TPP) followed by reduction to the amino group by using the literature method (see Supporting Information).[38] The product with *cis(syn)* configuration of the bis-substituted porphyrin (**H_2P-[NH_2]$_2$**: aminophenyl groups at the 5- and 10-positions of the porphyrin ring) was isolated by column chromatography on silica gel. The Zn complexes of these precursors were connected to the corresponding phenylazomethine dendrons (**D*n***: $n=1$–4) by using $TiCl_4$ as dehydrating reagent. Dendrons of various generations were synthesized by the established procedure.[39] These products were isolated and purified by column chromatography on silica gel and preparative HPLC on size-exclusion chromatography (SEC) columns. The fully dendronized zinc–porphyrins (**ZnP-[D*n*]$_4$**) were also prepared by the reported method.

All compounds were characterized by MADLI-TOF MS and ^{1}H NMR and ^{13}C NMR spectroscopy. The MS results clearly show the monodisperse molecular weight of these compounds in accordance with the theoretical masses (Supporting Information). In the ^{1}H NMR spectra, each signal for the dendrons and the porphyrin core (β protons on the pyrrole moieties) were identified at different chemical shifts. The β-proton signal ($\delta=8.7$ ppm) indicates structural symmetry around the porphyrin core. For example, **ZnP-[D4]$_4$** showed a singlet at $\delta=8.77$ ppm that indicates a symmetric conformation around the porphyrin core. The slight peak broadening relative to standard zinc–porphyrin compounds is due to the short spin–spin relaxation time T_2 resulting from the large encapsulating effect.[40] The β-proton signals of the mono-, bis-, and tris-substituted compounds **ZnP-[D4]$_m$** ($m=1$–3) were split into multiple peaks, because the symmetry of the molecular topology was lost (Figure 1). In principle, four doublets would be observed for **ZnP-[D4]$_1$** and **ZnP-[D4]$_3$**. Similarly, two singlets and two doublets would be observed for **ZnP-[D4]$_2$**. This is actually observed in the experimental spectra for **ZnP-[D4]$_2$** and **ZnP-[D4]$_3$**. However, **ZnP-[D4]$_1$** displayed a broad peak in which the signals are not separately identifiable. This indicates free rotation of the dendron groups on the NMR timescale. For the third-generation dendrimers **ZnP-[D3]$_m$**, no peak splitting was observed even in the bis- and tris-substituted compounds ($m=2$ and 3). In fact, all the conformations of these high-generation ($n=4$) compounds with $m=2$–4 dendrons are fixed due to the rigid π-conjugated backbone and large steric effect. The factor controlled by these numbers (m, n) is important for their molecular dynamics in the solution phase.

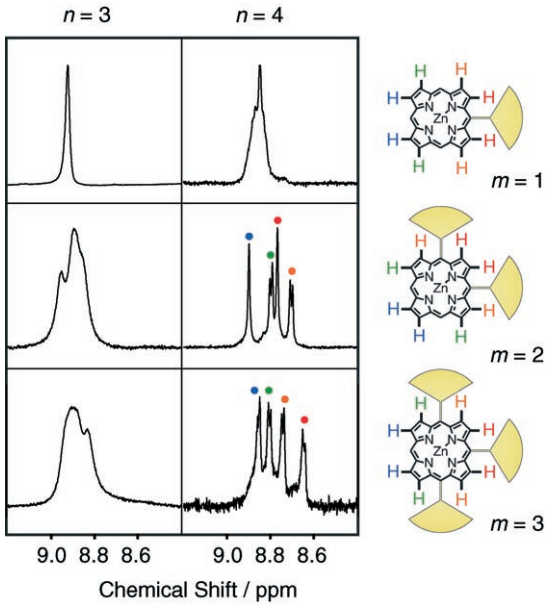

Figure 1. ^{1}H NMR spectra of DPAs in $CDCl_3$ focusing on β-protons at the porphyrin core.

Hydrodynamic properties of the dendrimers: The hydrodynamic properties of the fully substituted DPAs with a porphyrin core were determined on the basis of experimental data (Table 1). The partially substituted DPAs ($m=1$–3) were also studied on the basis of experimentally obtained intrinsic viscosity [η]. The fully ($m=4$) and partially ($m=2$, 3) substituted dendrimers have [η] values that parallel each other. For example, the bis-substituted DPA with four generations of dendrons **ZnP-[D4]$_2$** and the fully substituted DPA with three generations **ZnP-[D3]$_4$** have similar [η] values, which indicate similar hydrodynamic properties (radius, volume, or molecular density). An exception is the monosubstituted DPA, the [η] value of which is smaller. This means that the density of the monosubstituted DPA molecule is higher than those of the others because the [η] value is proportional to V_h/M_w, in which V_h is the hydrodynamic volume.[41] In other words, the free space (volume) inside the monosubstituted dendrimer is smaller.

Free volumes V_{free} were estimated by subtraction of van der Waals volumes V_{VW} from V_h. The calculated fractions of free space in the entire hydrodynamic volume (V_{free}/V_h) clearly demonstrated the differences between the monosubstituted dendrimer ($m=1$) and the others. The V_{free}/V_h of **ZnP-[D4]$_1$** was estimated to be 72%, while those of **ZnP-[D4]$_2$**, **ZnP-[D4]$_3$** and **ZnP-[D4]$_4$** were both 78%. According to NMR measurements, **ZnP-[D4]$_1$** could be in a bent conformation with free rotation of the dendron group. The smaller free space in **ZnP-[D4]$_1$** is consistent with the NMR result. In contrast, the multisubstituted DPAs ($m=2$–4) prevent backfolding and fix the dendron unit with retention of the nanospace around the core. In both cases, the DPAs have a relatively stiff backbone, as was shown by the larger free volumes. The DPAs with a zinc–porphyrin core retain a much larger free space than aryl ether dendrimers with the same core unit and number of branching generations. For example, the fully substituted aryl ether dendrimer with four generations of dendrons retains 45% free volume per unit hydrodynamic volume,[42] much smaller than that in the DPA architecture (78%). The difference between these dendrimers indicates effective restriction of backfolding in the DPA due to its rigid backbone. This also means that the layer-by-layer cascade topology of the dendrimer is main-

Table 1. Physical properties of the DPAs with a zinc–porphyrin core. The data of fully-substituted dendrimers ($m=4$) are from a previous paper.[24]

Compound	m[a]	n[b]	$[\eta]$[c] [dL g^{-1}]	V_h[d] [Å^3]	V_{free}[e] [Å^3]	V_{free}/V_h [%]	NMR[f]	N (n)[g]
ZnP-[D1]$_1$	1	1	0.0350	1990	1280	64.4	br	1 (1)
-[D2]$_1$	1	2	0.0401	3230	2200	68.2	br	1 (2)
-[D3]$_1$	1	3	0.0467	5990	4330	72.2	br	– (3)
-[D4]$_1$	1	4	0.0473	10600	7670	72.3	br	– (4)
ZnP-[D1]$_2$	2	1	0.0377	2590	1720	66.5	br	1 (1)
-[D2]$_2$	2	2	0.0458	5320	3820	71.7	br	1 (2)
-[D3]$_2$	2	3	0.0555	11700	8920	76.3	br	– (3)
-[D4]$_2$	2	4	0.0601	24200	18900	78.0	s, s, d, d	**4 (4)**
ZnP-[D1]$_3$	3	1	0.0419	3380	2350	69.6	br	1 (1)
-[D2]$_3$	3	2	0.0528	8020	6040	75.3	br	1 (2)
-[D3]$_3$	3	3	0.0598	17600	13700	77.9	br	– (3)
-[D4]$_3$	3	4	0.0603	35000	27300	78.0	d, d, d, d	**4 (4)**
ZnP-[D1]$_4$	4	1	0.0405	3750	2570	68.4	s	1 (1)
-[D2]$_4$	4	2	0.0534	10000	7580	75.5	s	1 (2)
-[D3]$_4$	4	3	0.0592	22400	17400	77.7	s	**3 (3)**
-[D4]$_4$	4	4	0.0591	44900	34800	77.5	s	**4 (4)**

[a] Number of dendrons. [b] Number of generations. [c] Intrinsic viscosity. [d] Hydrodynamic volume. [e] Free volume within the molecular hydrodynamic radius ($V_{free}=V_h-V_{VW}$). [f] ^{1}H NMR signals of the β-protons on the porphyrin ring. [g] Number of isosbestic points observed during UV/Vis titration with $SnCl_2$ (numbers in the parentheses are the ideal numbers for the complete stepwise processes), and bold face indicates cases in which ideal stepwise complexation was observed.

tained in the real conformational structure of the DPA, even in the solution phase. This structural character could be one of the important factors allowing stepwise layer-by-layer radial complexation without any distortion of the metal assembly.

These experimental results support the molecular models (Supporting Information) provided by optimizing calculations on these DPAs. The model of the fully substituted dendrimer **ZnP-[D4]$_4$** in particular predicts effective isolation of the porphyrin core from the external environment.[24] It was also shown that the dendrimer contains a large free volume in its dendritic shell. All models of the DPAs were generated by the same calculation procedure and adequately support all the obtained experimental data. Especially the asymmetric dendrimers with two or three dendrons retain their nanospace around the core in spite of their missing arms. However, monosubstituted **ZnP-[D4]$_1$** no longer retains the nanospace, and the porphyrin core is protrudes from the molecular cage. These structural characteristics are also supported by experimental data of their electrochemical behavior on an electrode surface. The standard electron-transfer kinetic constants $k°$ of the DPA series were determined by analyzing their cyclic voltammograms in THF. As shown in Figure 2, the porphyrin core in higher substituted dendrimers has a smaller $k°$ value. Although the kinetics on an electrode surface involve many factors, such as the electron transfer distance, adsorption equilibria, and environment around the redox center, it was definitely observed that the kinetics are attenuated by large substitution and generation numbers.[43–45] The half-wave redox potential $E_{1/2}$ of the zinc–porphyrin core also changed with generation number n and substitution number m. It is influenced by two effects of the dendrons: the direct electron-donating effect through covalent bonding, and the local-domain effect created by the encapsulating character of the dendrons. Increasing the generation number resulted in a continuous shift of $E_{1/2}$ for the multiply substituted DPAs. However, the $E_{1/2}$ of the monosubstituted DPAs ($m=1$) did not change while the generation number increased from $n=2$ to 4. These results suggesting absence of encapsulating character are consistent with the 3D model of **ZnP-[D4]$_1$**, which shows an open-shell configuration (Supporting Information).

It is known that dendritic encapsulation of the core induces a significant change in the redox potential.[46] This arises from noncovalent interaction between the redox center and the dendrons (or external environment). Fine-tuning of the nanospace inside the dendrimer could provide substrate specificity for molecular sensing.[47]

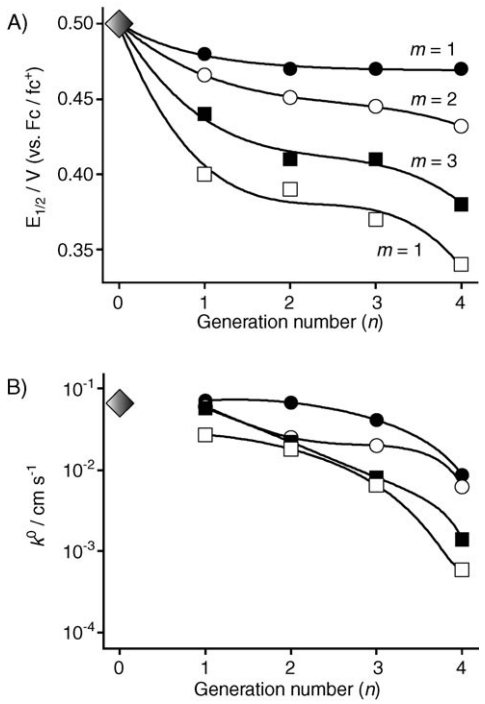

Figure 2. A) Standard redox potentials of the ZnP/ZnP$^+$ redox couple obtained from cyclic voltammograms of the DPAs. B) Standard rate constants of these redox reactions on a glassy carbon electrode in THF containing 0.1 mol L^{-1} Bu_4NPF_6 as supporting electrolyte. Data for the fully substituted DPA ($m=4$) were reported previously.[24]

Metal assembly in asymmetric DPAs: DPAs can generally assemble metallic compounds, such as $SnCl_2$[17] or $FeCl_3$.[24,48] All of the imino groups in each layer of the dendrimer are coordinating centers for these metal components. When 1:1 coordinating metals are selected, the number of coordination centers and assembled metal atoms would be identical. Previously, we confirmed stepwise radial complexation from the core to the outside layer in a fully substituted porphyrin-cored DPA (Scheme 2) by a spectroscopic investigation.

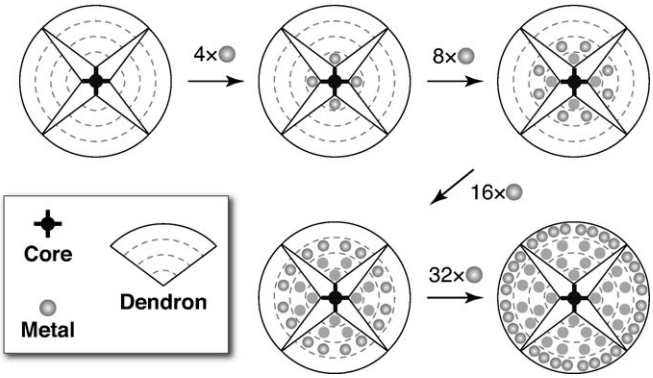

Scheme 2. Schematic representation of stepwise complexation in fully substituted phenylazomethine dendrimers with a zinc–porphyrin core.

Similarly, stepwise complexation in asymmetric DPAs is also expected, because this is mainly based on the electronic character of the dendrons. The complexation process of $SnCl_2$ to these dendrimers was determined by using the UV/Vis absorption spectra.

Complexation of $SnCl_2$ with the imino nitrogen atom of a phenylazomethine unit brings about changes in UV/Vis absorption, accompanied by an isosbestic point around 360 nm. If coordination were a random process with no interchromophore interaction, the isosbestic point should appear at only one wavelength. However, the isosbestic point is not necessarily fixed in the case of a nonuniformly coordinating system in which complexation to a specific center is preferred relative to the other centers. The DPAs have multiple coordinating centers in a cascade topology. A pair of centers in the same cascade layer is located in the same chemical environment, but the another center in a different layer is in a different environment. In particular, the DPAs have a highly graduated basicity of the coordinating center across these layers. As a result, stepwise complexation successively proceeds during the addition of small amounts of $SnCl_2$ until full complexation. This is a stoichiometric process due to the 1:1 complexation between the imine nitrogen atoms and $SnCl_2$. In this case, the isosbestic point should shift only when coordination switches to the next layer during titration.

Such observations were also confirmed during the titration of **ZnP-[D4]$_3$** and **ZnP-[D4]$_2$** (Figure 3). For example, the isosbestic point shifted when 3, 9, and 21 molar equivalents of $SnCl_2$ versus **ZnP-[D4]$_3$** were added. These quantities are in agreement with the number of coordination centers (imino groups) in the first, second, and third layers from the core of **ZnP-[D4]$_3$**. Bis-substituted **ZnP-[D4]$_2$** also displayed a stepwise shift, which suggests possible metal assembly in a stepwise fashion even in asymmetric DPAs. However, the monosubstituted porphyrin **ZnP-[D4]$_1$** has disordered metal-assembling behavior (Scheme 3). During the titration of **ZnP-[D4]$_1$** by $SnCl_2$, more than four isosbestic points were observed. The DPAs with three generations (**ZnP-[D3]$_m$**) were also studied (Supporting Information). Although complexation to give a fully substituted **ZnP-[D3]$_4$** is a three-step process from the core to the outside, the asymmetric series **ZnP-[D3]$_m$** ($m=1$–3) did not show a definite isosbestic point. It gradually shifted toward a shorter wavelength on titration.

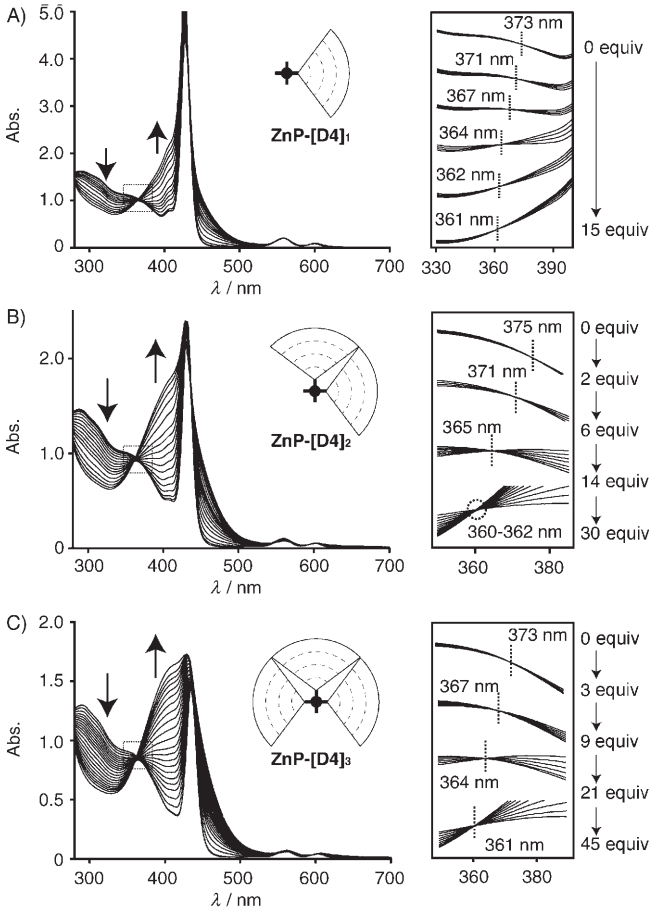

Figure 3. UV/Vis spectra for stepwise addition of $SnCl_2$ to a solution of A) **ZnP-[D4]$_1$**, B) **ZnP-[D4]$_2$**, and C) **ZnP-[D4]$_3$** in C_6H_6/CH_3CN (1:1).

Discussion

The relationship between structural character of the DPA and metal-assembling behavior was reconsidered. In summary, the backbone conformations of the multiply substituted dendrimers with four generations **ZnP-[D4]$_m$** ($m=2$–4) are rigid and fixed due to their self-fixation, while those of monosubstituted **ZnP-[D4]$_1$** and the DPAs with three genera-

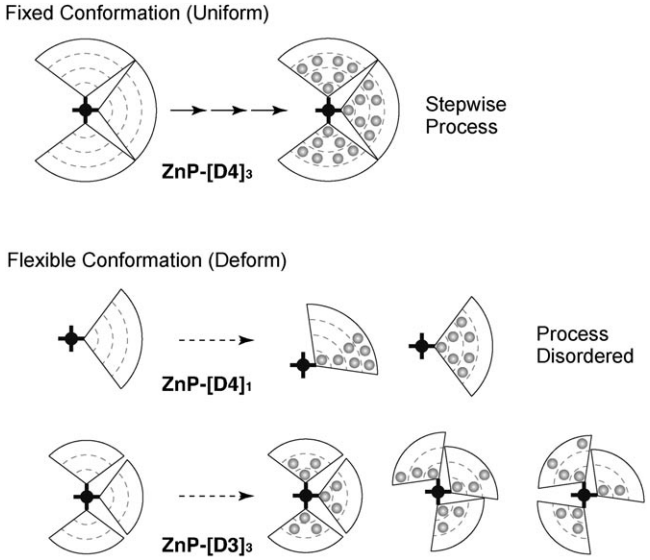

Scheme 3. Schematic representation of stepwise complexation in partially substituted phenylazomethine dendrimers with a zinc–porphyrin core.

tions (**ZnP-[D3]$_m$**: $m=1$–4) are not. There is a mutual relation between structural character and metal complexation. The group **ZnP-[D4]$_m$** ($m=2$–4), in which the conformation is fixed, is capable of finely controlled metal assembly from the core to the outside. In contrast, the other group (**ZnP-[D3]$_m$**: $m=1$–3) could not precisely control complexation.

In our previous study, a DPA with a monosubstituted phenyl group as core also exhibited similar stepwise complexation starting from the core.[16] It is likely that stepwise complexation is a characteristic property of the dendritic phenylazomethine block. Distortion of the inherent property gradient based on the electron density or donor strength should be due to the bent conformation toward the vacant space around the core unit. This could be confirmed by quantitative analysis of the free space inside the dendrimer structure. The smaller space in **ZnP-[D4]$_1$** ($V_{free}/V_h=72\,\%$) than in **ZnP-[D4]$_m$** ($V_{free}/V_h=78\,\%$) is direct evidence of the bent structure shown by the molecular models. The lost free volume in the DPA molecule should be equivalent to the nanospace around the porphyrin center. On the experimental side, six distinguishable isosbestic points were determined by careful observation in the UV/Vis spectra on the titration of **ZnP-[D4]$_1$**. A possible reason for the unusual titration behavior is loss of the structural symmetry due to the bent bridges and rotation of the core–dendron connection. Similar considerations are also applicable for the partially substituted asymmetric dendrimers with three generations (**ZnP-[D3]$_m$**: $m=1$–3). The ^{1}H NMR spectroscopic data indicate that the molecular conformations of these dendrimers are not fixed in solution at room temperature. The molecular dynamics strongly influence the finely controlled metal-assembling property of the DPA blocks. This idea is also supported by the indistinct isosbestic point during the titration of **ZnP-[D3]$_m$** ($m=1$–3).

Many dendritic multiligands are known, such as PAMAM and polypropyleneamine dendrimers. Although they can collect multiple metal ions in their vacant space, the detailed metal-assembling process could never be defined and recognized. It should be a random process because of their indefinite conformation and roughly even distribution of electronic density. These dendrimers have relatively flexible backbones. In contrast, DPAs have a rigid π-conjugated framework in which the electron-donating property of the imine units enhances electron density nearer the core. Not only the basicity factor, but also the fixed conformation due to stiff chemical bonding is a key property for finely controlled metal assembly in DPAs. This provides us with information about the molecular design strategy for novel metal-assembling materials.

Conclusion

An asymmetric series of dendritic phenylazomethines (DPAs) with a porphyrin core was synthesized to reveal the structural requirements for stepwise radial complexation. All the DPAs prepared in this study are macromolecular ligands capable of stoichiometric assembly of metal compounds. However, the stepwise reaction from the core to the outside proceeded successfully only in the multidendronized DPAs with four generations. This can be related to the static or dynamic conformation of the DPAs in solution. Dendrimers **ZnP-[D4]$_m$** ($m=2$–4) with finely controlled metal assembly have fixed conformations, at least on the NMR timescale. These dendrimers retain the nanospace created in the molecule without backfolding of the dendron termini. In contrast, the conformations of the distorted metal-assembling dendrimers (**ZnP-[D4]$_1$** and **ZnP-[D3]$_m$**: $m=1$–3) are not fixed. In these molecules, a topological layer-by-layer structure is not necessarily retained in the actual geometric space. Because identical coordinating environments in the same layer would be distorted, the ideal stepwise reaction is no longer feasible. This observation provides new insight into design strategy for finely controlled metal-assembling materials. The primary requirement is an intrinsic basicity gradient along the molecular cascades, which could be generated by amplification of the electron-donating/withdrawing property of the dendritic building blocks. The next requirement is conformational stability of the molecules in order to retain the unique layer-by-layer architecture.

Experimental Section

General methods: The NMR spectra were recorded on an FT-NMR spectrometer (JEOL, JNM-GX 400) operating at 400 MHz (^{1}H) or 100 MHz (^{13}C) at room temperature (25 °C). The ^{1}H NMR chemical shifts were referenced to the residual proton signal of $CDCl_3$ ($\delta=7.26$ ppm) and TMS ($\delta=0$ ppm) as internal standards. The ^{13}C NMR chemical shifts were referenced to $CDCl_3$ ($\delta=77.0$ ppm). The ^{1}H NMR pulse relaxation times T_1 were measured in the saturation–recovery data-processing mode. The MALDI-TOF mass spectra were obtained on a Shimadzu/Kratos

AXIMA CFR plus mass spectrometer in positive mode with dithranol (1,8-dihydroxy-9[10*H*]-anthracenone) as the matrix. Dendrimers were purified by preparative recycling HPLC (Japan Analytical Industry: LC908) with chloroform or THF as eluent at a flow rate of 3.5 mL min^{-1}.

Materials: Titanium(IV) chloride ($TiCl_4$), 1,4-diazabicyclo[2.2.2]octane (DABCO), benzophenone, chlorobenzene, and all solvents used for the purifications were purchased from Kantoh Kagaku Co. All other solvents for the measurements were of dehydrated grade for organic synthesis from Kantoh Kagaku Co. The partially substituted aminophenyl porphyrins as precursors of the dendrimer core were synthesized by a modified literature method (see Supporting Information). All DPA dendrons (G2–G4) were synthesized as previously described.[39] All fully substituted DPAs with a zinc–porphyrin core (**ZnP-[D*n*]$_4$**: $n=1$–4) were prepared by a previously reported method.[24]

General synthetic procedure for partially dendronized porphyrin (ZnP-[D*n*]$_m$): Aminophenylporphyrin **H$_2$P-[NH$_2$Ph]$_m$** was treated with an excess of anhydrous $ZnCl_2$ in refluxing THF under an N_2 atmosphere for 3 h. The resulting mixture was concentrated, and the product precipitated with distilled water and collected by filtration to obtain **ZnP-[NH$_2$Ph]$_m$** as a purple solid. The crude product was used for the next reaction after washing with water. **ZnP-[NH$_2$Ph]$_m$**, DABCO, and the corresponding DPA dendron (generation number *n*) were dissolved in chlorobenzene (15 mL). $TiCl_4$ (dehydrating reagent) was added through a dropping funnel as a 1:4 solution in chlorobenzene. The reaction mixture was heated at 125 °C for 2 h. It was then filtered, and the solution concentrated to dryness. The dendrimer products **ZnP-[D*n*]$_m$** were isolated by chromatography on a silica-gel column with hexane/chloroform/ethyl acetate as eluent in the presence of 0.5 % triethylamine and purified by preparative recycling HPLC with THF as eluent.

Synthesis of ZnP-[D1]$_1$: Porphyrin **H$_2$P-[NH$_2$Ph]$_1$** (50 mg, 0.072 mmol), benzophenone (G1, 53 mg, 0.29 mmol), DABCO (250 mg, 2.2 mmol), and $TiCl_4$ (60 μL, 0.55 mmol) were used for the synthesis. A 25 mg (54 %) amount of product was isolated after purification. ^{1}H NMR (400 MHz, $CDCl_3$, 25 °C, TMS): $\delta=8.94$–8.86 (br, 8H; pyrrole), 8.20 (br, 6H), 7.94–7.38 (m, 21H), 7.07 ppm (d, $J=7.8$ Hz, 2H); ^{13}C NMR (100 MHz, $CDCl_3$, 25 °C): $\delta=169.15$, 150.93, 150.21, 150.03, 142.75, 139.40, 137.49, 136.35, 134.31, 131.82, 130.89, 129.80, 129.43, 128.89, 128.27, 127.94, 127.37, 126.44, 120.92, 119.04 ppm; MALDI-TOF-MS (dithranol): *m/z* calcd: 856.24 $[M+H]^+$, found: 856.39; UV/Vis ($CHCl_3$/CH_3CN 1/1): λ_{max} ($\lg\varepsilon$) = 315 (4.287), 425 (5.747), 557 (4.297), 599 nm (3.922).

Synthesis of ZnP-[D2]$_1$: Porphyrin **H$_2$P-[NH$_2$Ph]$_1$** (50 mg, 0.072 mmol), G2 dendron (157 mg, 0.29 mmol), DABCO (250 mg, 2.2 mmol), and $TiCl_4$ (60 μL, 0.55 mmol) were used for the synthesis. A 33 mg (50 %) amount of product was isolated after purification. ^{1}H NMR (400 MHz, $CDCl_3$, 25 °C, TMS): $\delta=8.93$ (br, 8H; pyrrole), 8.20 (br, 6H), 7.92 (br, 2H), 7.80–6.59 ppm (m, 39H); ^{13}C NMR (100 MHz, $CDCl_3$, 25 °C): $\delta=168.2$, 168.44, 168.36, 153.65, 152.04, 151.00, 150.24, 150.02, 142.74, 142.72, 139.31, 139.11, 137.18, 135.85, 135.61, 134.68, 134.44, 134.32, 131.80, 130.90, 130.65, 130.16, 129.45, 129.38, 129.31, 129.25, 128.84, 128.42, 128.19, 128.16, 128.06, 127.62, 127.36, 126.44, 120.60, 120.23, 119.46 ppm; MALDI-TOF-MS (dithranol): *m/z* calcd: 1216.77 $[M+H]^+$, found: 1216.67; UV/Vis ($CHCl_3$/CH_3CN 1/1) λ_{max} ($\lg\varepsilon$) = 287 (4.683), 422 (5.694), 558 (4.301), 599 nm (3.950).

Synthesis of ZnP-[D3]$_1$: Porphyrin **H$_2$P-[NH$_2$Ph]$_1$** (50 mg, 0.072 mmol), G3 dendron (364 mg, 0.29 mmol), DABCO (250 mg, 2.2 mmol), and $TiCl_4$ (60 μL, 0.55 mmol) were used for the synthesis. A 52 mg (48 %) amount of the product was isolated after purification. ^{1}H NMR (400 MHz, $CDCl_3$, 25 °C, TMS): $\delta=8.93$ (br, 8H; pyrrole), 8.21 (br, 6H), 7.97 (d, $J=7.8$ Hz, 2H), 7.78–6.61 (m, 71H), 6.50 (d, $J=7.6$ Hz, 2H), 6.29 ppm (d, $J=8.4$ Hz, 2H); ^{13}C NMR (100 MHz, $CDCl_3$, 25 °C): $\delta=168.95$, 168.58, 168.45, 168.37, 168.18, 168.11, 154.12, 153.73, 153.66, 152.45, 151.90, 151.53, 151.29, 150.02, 149.93, 142.79, 142.73, 139.26, 139.07, 137.98, 137.26, 135.78, 135.60, 135.32, 134.39, 134.24, 134.19, 131.79, 130.89, 130.61, 130.46, 130.35, 130.11, 129.41, 128.91, 128.82, 128.40, 128.18, 128.02, 127.91, 127.54, 127.35, 126.45, 121.22, 120.91, 120.67, 120.52, 120.32, 120.01, 119.55 ppm; MALDI-TOF-MS (dithranol): *m/z* calcd: 1933.64 $[M+H]^+$, found: 1932.88; UV/Vis ($CHCl_3$/CH_3CN 1/1): λ_{max} ($\lg\varepsilon$) = 291 (4.927), 423 (5.710), 558 (4.279), 599 nm (3.919).

Synthesis of ZnP-[D4]$_1$: Porphyrin **H$_2$P-[NH$_2$Ph]$_1$** (40 mg, 0.058 mmol), G4 dendron (100 mg, 0.037 mmol), DABCO (251 mg, 2.2 mmol), and $TiCl_4$ (30 μL, 0.27 mmol) were used for the synthesis. An 80 mg (75 %) amount of product was isolated after purification. ^{1}H NMR (400 MHz, $CDCl_3$, 25 °C, TMS): $\delta=8.85$ (br, 8H; pyrrole), 8.13 (br, 6H), 7.87–6.57 ppm (m, 149H); ^{13}C NMR (100 MHz, $CDCl_3$, 25 °C): $\delta=169.05$, 168.82, 168.56, 168.35, 168.20, 168.08, 153.82, 152.01, 150.03, 142.87, 139.33, 135.85, 135.65, 134.50, 133.46, 132.41, 131.77, 130.97, 130.47, 130.16, 130.06, 129.44, 128.86, 128.24, 128.06, 127.88, 126.46, 122.24, 120.91, 120.56, 120.35, 119.48, 118.11 ppm; MALDI-TOF-MS (dithranol): *m/z* calcd: 3367.38 $[M+H]^+$, found: 3367.42; UV/Vis ($CHCl_3$/CH_3CN 1/1): λ_{max} ($\lg\varepsilon$) = 291 (5.191), 427 (5.637), 558 (4.293), 600 nm (3.950).

Synthesis of ZnP-[D1]$_2$: Porphyrin **H$_2$P-[NH$_2$Ph]$_2$** (75 mg, 0.11 mmol), benzophenone (G1, 58 mg, 0.32 mmol), DABCO (250 mg, 2.2 mmol), and $TiCl_4$ (60 μL, 0.55 mmol) were used for the synthesis. A 73 mg (73 %) amount of the product was isolated after purification. ^{1}H NMR (400 MHz, $CDCl_3$, 25 °C, TMS): $\delta=8.91$–8.83 (br, 8H; pyrrole), 8.81 (br, 4H), 7.96–6.98 ppm (m, 34H); ^{13}C NMR (100 MHz, $CDCl_3$, 25 °C): $\delta=169.14$, 150.91, 150.00, 143.01, 142.77, 139.42, 137.54, 136.38, 135.65, 134.28, 131.65, 130.90, 129.81, 129.43, 128.88, 128.28, 128.16, 127.96, 127.31, 126.40, 125.45, 120.77, 119.00 ppm; MALDI-TOF-MS (dithranol): *m/z* calcd: 1037.55 $[M+H]^+$, found: 1037.48; UV/Vis ($CHCl_3$/CH_3CN 1/1): λ_{max} ($\lg\varepsilon$) = 313 (4.345), 429 (5.606), 559 (4.298), 601 nm (4.017).

Synthesis of ZnP-[D2]$_2$: Porphyrin **H$_2$P-[NH$_2$Ph]$_2$** (60 mg, 0.085 mmol), G2 dendron (138 mg, 0.26 mmol), DABCO (250 mg, 2.2 mmol), and $TiCl_4$ (60 μL, 0.55 mmol) were used for the synthesis. An 88 mg (64 %) amount of the product was isolated after purification. ^{1}H NMR (400 MHz, $CDCl_3$, 25 °C, TMS): $\delta=8.91$ (br, 8H; pyrrole), 8.21 (br, 4H), 7.93 (br, 4H), 7.81–6.75 (m, 64H), 6.57 ppm (br, 2H); ^{13}C NMR (100 MHz, $CDCl_3$, 25 °C): $\delta=168.88$, 168.44, 153.63, 152.03, 150.96, 150.23, 149.91, 142.77, 139.32, 139.05, 137.21, 135.85, 135.60, 134.71, 134.47, 134.33, 131.87, 131.75, 130.89, 130.61, 130.16, 129.97, 129.46, 129.39, 129.30, 129.24, 128.85, 128.39, 128.18, 128.16, 128.05, 127.59, 127.32, 126.42, 120.57, 120.22, 119.49 ppm; MALDI-TOF-MS (dithranol): *m/z* calcd: 1754.42 $[M+H]^+$, found: 1753.81; UV/Vis ($CHCl_3$/CH_3CN 1/1): λ_{max} ($\lg\varepsilon$) = 286 (4.920), 428 (5.699), 559 (4.327), 601 nm (4.064).

Synthesis of ZnP-[D3]$_2$: Porphyrin **H$_2$P-[NH$_2$Ph]$_2$** (45 mg, 0.064 mmol), G3 dendron (240 mg, 0.19 mmol), DABCO (250 mg, 2.2 mmol), and $TiCl_4$ (60 μL, 0.55 mmol) were used for the synthesis. A 107 mg (58 %) amount of the product was isolated after purification. ^{1}H NMR (400 MHz, $CDCl_3$, 25 °C, TMS): $\delta=8.96$–8.89 (br, 8H; pyrrole), 8.18 (br, 4H), 7.96 (br, 4H), 7.78–6.70 (m, 122H), 6.62 (d, $J=8.0$ Hz, 8H), 6.49 (d, $J=5.6$ Hz, 4H), 6.31 ppm (d, $J=8.4$ Hz, 4H); ^{13}C NMR (100 MHz, $CDCl_3$, 25 °C): $\delta=168.94$, 168.56, 168.45, 168.32, 168.13, 168.06, 154.08, 153.72, 153.66, 152.45, 151.91, 151.56, 150.96, 150.14, 149.80, 142.83, 139.26, 139.07, 137.35, 135.79, 135.75, 135.59, 135.32, 134.47, 134.38, 134.28, 134.19, 131.88, 131.59, 130.87, 130.59, 130.43, 130.35, 130.18, 130.11, 129.41, 129.38, 128.91, 128.84, 128.39, 128.17, 128.02, 127.92, 127.53, 127.31, 126.40, 120.90, 120.71, 120.52, 120.31, 120.00, 119.59 ppm; MALDI-TOF-MS (dithranol): *m/z* calcd: 3188.16 $[M+H]^+$, found: 3186.84; UV/Vis ($CHCl_3$/CH_3CN 1/1): λ_{max} ($\lg\varepsilon$) = 292 (5.187), 429 (5.691), 559 (4.325), 601 nm (4.054).

Synthesis of ZnP-[D4]$_2$: Porphyrin **H$_2$P-[NH$_2$Ph]$_2$** (30 mg, 0.043 mmol), G4 dendron (360 mg, 0.13 mmol), DABCO (250 mg, 2.2 mmol), and $TiCl_4$ (60 μL, 0.55 mmol) were used for the synthesis. A 160 mg (68 %) amount of the product was isolated after purification. ^{1}H NMR (400 MHz, $CDCl_3$, 25 °C, TMS): $\delta=8.91$ (s, 2H; pyrrole), 8.80 (d, $J=4.4$ Hz, 2H; pyrrole), 8.78 (s, 2H; pyrrole), 8.71 (d, $J=4.4$ Hz, 2H; pyrrole), 8.04 (d, $J=7.2$ Hz, 4H), 7.82–6.54 (m, 266H), 6.36 (d, $J=6.8$ Hz, 4H), 6.24 (d, $J=7.2$ Hz, 4H), 6.05 (d, $J=7.6$ Hz, 4H), 6.01 (d, $J=8.0$ Hz, 4H), 5.74 ppm (d, $J=6.8$ Hz, 4H); ^{13}C NMR (100 MHz, $CDCl_3$, 25 °C): $\delta=168.88$, 168.40, 168.34, 168.17, 167.99, 167.85, 167.78, 153.91, 153.70, 153.29, 151.91, 151.40, 151.16, 150.16, 149.88, 139.23, 139.15, 138.94, 138.87, 135.78, 135.54, 135.18, 134.43, 134.24, 131.93, 130.89, 130.61, 130.38, 130.09, 129.87, 129.71, 129.40, 129.06, 128.82, 128.17, 127.99, 127.88, 127.76, 126.27, 121.26, 120.71, 120.48, 120.26, 120.06, 119.44 ppm; MALDI-TOF-MS (dithranol): *m/z* calcd: 6055.64 $[M+H]^+$, found:

6055.77; UV/Vis ($CHCl_3/CH_3CN$ 1/1): λ_{max} ($\lg\varepsilon$) = 289 (5.468), 432 (5.679), 560 (4.294), 602 nm (4.046).

Synthesis of ZnP-[D1]$_3$: Porphyrin **H$_2$P-[NH$_2$Ph]$_3$** (50 mg, 0.069 mmol), benzophenone (G1, 63 mg, 0.35 mmol), DABCO (250 mg, 2.2 mmol), and $TiCl_4$ (60 μL, 0.55 mmol) were used for the synthesis. A 15 mg (19%) amount of the product was isolated after purification. ^{1}H NMR (400 MHz, $CDCl_3$, 25°C, TMS): δ = 8.90–8.82 (br, 8H; pyrrole), 8.20 (br, 2H), 7.97–7.42 (m, 37H), 7.08 ppm (br, 8H); ^{13}C NMR (100 MHz, $CDCl_3$, 25°C): δ = 168.88, 168.40, 168.34, 168.17, 167.99, 167.85, 167.78, 153.91, 153.70, 153.29, 151.91, 151.40, 151.16, 150.16, 149.88, 139.23, 139.15, 138.94, 138.87, 135.78, 135.54, 135.18, 134.43, 134.24, 131.93, 130.89, 130.61, 130.38, 130.09, 129.87, 129.71, 129.40, 129.06, 128.82, 128.17, 127.99, 127.88, 127.76, 126.27, 121.26, 120.71, 120.48, 120.26, 120.06, 119.44 ppm; MALDI-TOF-MS (dithranol): *m/z* calcd: 6055.64 $[M+H]^+$, found: 6055.77; UV/Vis ($CHCl_3/CH_3CN$ 1/1): λ_{max} ($\lg\varepsilon$) = 312 (4.437), 429 (5.763), 559 (4.351), 601 nm (4.111).

Synthesis of ZnP-[D2]$_3$: Porphyrin **H$_2$P-[NH$_2$Ph]$_3$** (40 mg, 0.056 mmol), G2 dendron (150 mg, 0.28 mmol), DABCO (250 mg, 2.2 mmol), and $TiCl_4$ (60 μL, 0.55 mmol) were used for the synthesis. A 72 mg (67%) amount of the product was isolated after purification. ^{1}H NMR (400 MHz, $CDCl_3$, 25°C, TMS): δ = 8.56 (br, 8H; pyrrole), 7.82–6.72 (m, 97H), 6.47 ppm (m, 4H); ^{13}C NMR (100 MHz, $CDCl_3$, 25°C): δ = 168.83, 168.78, 168.40, 168.23, 153.57, 152.00, 150.72, 149.74, 149.68, 149.44, 142.87, 139.35, 139.01, 137.38, 135.85, 135.60, 134.74, 134.32, 131.32, 130.88, 130.54, 130.14, 129.47, 129.39, 129.29, 129.19, 128.87, 128.17, 128.06, 127.53, 127.08, 126.18, 120.57, 120.26, 120.16, 119.23 ppm; MALDI-TOF-MS (dithranol): *m/z* calcd: 2292.07 $[M+H]^+$, found: 2292.87; UV/Vis ($CHCl_3/CH_3CN$ 1/1): λ_{max} ($\lg\varepsilon$) = 285 (5.056), 432 (5.716), 560 (4.338), 602 nm (4.142).

Synthesis of ZnP-[D3]$_3$: Porphyrin **H$_2$P-[NH$_2$Ph]$_3$** (30 mg, 0.042 mmol), G3 dendron (261 mg, 0.48 mmol), DABCO (250 mg, 2.2 mmol), and $TiCl_4$ (60 μL, 0.55 mmol) were used for the synthesis. A 97 mg (62%) amount of the product was isolated after purification. ^{1}H NMR (400 MHz, $CDCl_3$, 25°C, TMS): δ = 8.91–8.84 (br, 8H; pyrrole), 8.15 (br, 2H), 7.95 (br, 6H), 7.78–6.51 (m, 193H), 6.31 ppm (d, J = 7.2 Hz, 8H); ^{13}C NMR (100 MHz, $CDCl_3$, 25°C): δ = 168.92, 168.54, 168.44, 168.31, 168.10, 168.01, 154.05, 153.70, 153.66, 152.42, 151.89, 151.57, 150.90, 150.01, 139.26, 139.06, 137.48, 135.79, 135.73, 135.58, 135.32, 134.51, 134.39, 134.29, 134.19, 134.10, 131.63, 130.85, 130.61, 130.44, 130.34, 130.10, 129.40, 129.36, 128.92, 128.83, 128.40, 128.16, 128.02, 128.92, 128.54, 128.39, 120.88, 120.72, 120.50, 120.30, 120.00, 119.59 ppm; MALDI-TOF-MS (dithranol): *m/z* calcd: 4442.68 $[M+H]^+$, found: 4440.21; UV/Vis ($CHCl_3/CH_3CN$ 1/1): λ_{max} ($\lg\varepsilon$) = 291 (5.344), 433 (5.701), 560 (4.333), 603 nm (4.124).

Synthesis of ZnP-[D4]$_3$: Porphyrin **H$_2$P-[NH$_2$Ph]$_3$** (50 mg, 0.069 mmol), the G4 dendron (1.00 g, 0.37 mmol), DABCO (250 mg, 2.2 mmol), and $TiCl_4$ (100 μL, 0.91 mmol) were used for the synthesis. A 242 mg (43%) amount of product was isolated after purification. ^{1}H NMR (400 MHz, $CDCl_3$, 25°C, TMS): δ = 8.87 (d, J = 4.0 Hz, 2H; pyrrole), 8.81 (d, J = 4.0 Hz, 2H; pyrrole), 8.75 (d, J = 4.4 Hz, 2H; pyrrole), 8.66 (d, J = 4.0 Hz, 2H; pyrrole), 7.97–6.06 (m, 423H), 5.83 (d, J = 8.0 Hz, 2H); ^{13}C NMR (100 MHz, $CDCl_3$, 25°C): δ = 169.11, 168.87, 168.36, 168.13, 167.84, 153.69, 151.90, 139.27, 135.76, 135.56, 130.88, 130.60, 130.37, 130.09, 129.36, 129.09, 128.80, 128.18, 128.00, 127.88, 127.82, 127.53, 121.10, 120.90, 120.49, 120.24, 120.05 ppm; MALDI-TOF-MS (dithranol): *m/z* calcd: 8743.90 $[M+H]^+$, found: 8743.00; UV/Vis ($CHCl_3/CH_3CN$ 1/1): λ_{max} ($\lg\varepsilon$) = 290 (5.643), 434 (5.687), 560 (4.315), 602 nm (4.108).

Acknowledgements

This work was supported in part by the Core Research for Evolutional Science and Technology (CREST) program of the Japan Science and Technology (JST) Agency, and by a Scientific Research Program for the 21st Century Center of Excellence (COE) (Keio-LCC) of the Ministry of Education, Culture, Sports, Science and Technology (MEXT) of Japan.

[1] D. Astruc, F. Lu, J. R. Aranzaes, *Angew. Chem.* **2005**, *117*, 8062–8083; *Angew. Chem. Int. Ed.* **2005**, *44*, 7852–7872.
[2] R. Shenhar, T. B. Norsten, V. M. Rotello, *Adv. Mater.* **2005**, *17*, 657–669.
[3] B. L. Cushing, V. L. Kolesnichenko, C. J. O'Connor, *Chem. Rev.* **2004**, *104*, 3893–3964.
[4] V. Vicinelli, P. Ceroni, M. Maestri, V. Balzani, M. Gorka, F. Vögtle, *J. Am. Chem. Soc.* **2002**, *124*, 6461–6468.
[5] F. L. Derf, E. Levillain, G. Trippé, A. Gorgues, M. Sallé, R.-M. Sebastían, A.-M. Caminade, J.-P. Majoral, *Angew. Chem.* **2001**, *113*, 230–233; *Angew. Chem. Int. Ed.* **2001**, *40*, 224–227.
[6] M. Tominaga, J. Hosogi, K. Konishi, T. Aida, *Chem. Commun.* **2000**, 719–720.
[7] F. Vögtle, S. Gestermann, C. Kauffmann, P. Ceroni, V. Vicinelli, V. Balzani, *J. Am. Chem. Soc.* **2000**, *122*, 10398–10404.
[8] M. F. Ottaviani, F. Montalti, N. J. Turro, D. A. Tomalia, *J. Phys. Chem. B* **1997**, *101*, 158–166.
[9] R. M. Crooks, M. Zhao, L. Sun, V. Chechik, L. K. Yeung, *Acc. Chem. Res.* **2001**, *34*, 181–190.
[10] S. Kéki, J. Török, G. Deák, L. Daróczi, M. Zsuga, *J. Colloid Interface Sci.* **2000**, *229*, 550–553.
[11] Y. Nakanishi, T. Imae, *J. Colloid Interface Sci.* **2005**, *285*, 158–162.
[12] X. Sun, S. Dong, E. Wang, *Macromolecules* **2004**, *37*, 7105–7108.
[13] H. Ye, R. M. Crooks, *J. Am. Chem. Soc.* **2005**, *127*, 4930–4934.
[14] M. Zhao, R. M. Crooks, *Adv. Mater.* **1999**, *11*, 217–220.
[15] M. Zhao, R. M. Crooks, *Angew. Chem.* **1999**, *111*, 375–377; *Angew. Chem. Int. Ed.* **1999**, *38*, 364–366.
[16] K. Yamamoto, T. Imaoka, *Bull. Chem. Soc. Jpn.* **2006**, *79*, 511–526.
[17] K. Yamamoto, M. Higuchi, S. Shiki, M. Tsuruta, H. Chiba, *Nature* **2002**, *415*, 509–511.
[18] T. Imaoka, H. Horiguchi, K. Yamamoto, *J. Am. Chem. Soc.* **2003**, *125*, 340–341.
[19] N. Satoh, J.-S. Cho, M. Higuchi, K. Yamamoto, *J. Am. Chem. Soc.* **2003**, *125*, 8104–8105.
[20] M. Higuchi, M. Tsuruta, H. Chiba, S. Shiki, K. Yamamoto, *J. Am. Chem. Soc.* **2003**, *125*, 9988–9997.
[21] O. Enoki, T. Imaoka, K. Yamamoto, *Org. Lett.* **2003**, *5*, 2547–2549.
[22] A. Kimoto, K. Masachika, J.-S. Cho, M. Higuchi, K. Yamamoto, *Org. Lett.* **2004**, *6*, 1179–1182.
[23] N. Satoh, T. Nakashima, K. Yamamoto, *J. Am. Chem. Soc.* **2005**, *127*, 13030–13038.
[24] T. Imaoka, R. Tanaka, S. Arimoto, M. Sakai, M. Fujii, K. Yamamoto, *J. Am. Chem. Soc.* **2005**, *127*, 13896–13905.
[25] O. Enoki, H. Katoh, K. Yamamoto, *Org. Lett.* **2006**, *8*, 569–571.
[26] W. Oriz, A. E. Roitberg, J. L. Krause, *J. Phys. Chem. B* **2004**, *108*, 8218–8225.
[27] M. Han, P. Chen, X. Yang, *Polymer* **2005**, *46*, 3481–3488.
[28] P. K. Maiti, T. Çağin, G. Wang, W. A. Goddard III, *Macromolecules* **2004**, *37*, 6236–6254.
[29] D. Boris, M. Rubinstein, *Macromolecules* **1996**, *29*, 7251–7260.
[30] M. Chai, Y. Niu, W. J. Youngs, P. L. Rinaldi, *J. Am. Chem. Soc.* **2001**, *123*, 4670–4678.
[31] D. Pötschke, M. Ballauff, P. Lindner, M. Fischer, F. Vögtle, *Macromolecules* **1999**, *32*, 4079–4087.
[32] M. Ballauff, *Top. Curr. Chem.* **2001**, *212*, 177–194.
[33] M. Ballauff, C. N. Likos, *Angew. Chem.* **2004**, *116*, 3060–3082; *Angew. Chem. Int. Ed.* **2004**, *43*, 2998–3020.
[34] S. Rosenfeldt, N. Dingenouts, D. Pötschke, M. Ballauff, A. J. Berresheim, K. Müllen, P. Lindner, *Angew. Chem.* **2004**, *116*, 111–114; *Angew. Chem. Int. Ed.* **2004**, *43*, 109–112.
[35] M. Wind, K. Saalwächter, U.-M. Wiesler, K. Müllen, H. W. Spiess, *Macromolecules* **2002**, *35*, 10071–10086.
[36] M. Higuchi, S. Shiki, K. Ariga, K. Yamamoto, *J. Am. Chem. Soc.* **2001**, *123*, 4414–4420.
[37] D.-L. Jiang, T. Aida, *J. Am. Chem. Soc.* **1998**, *120*, 10895–10901.
[38] W. J. Kruper, T. A. Chamberlin, Jr., M. Kochanny, *J. Org. Chem.* **1989**, *54*, 2753–2756.

[39] K. Takanashi, H. Chiba, M. Higuchi, K. Yamamoto, *Org. Lett.* **2004**, *6*, 1709–1712.
[40] D. D. Traficante in *Encyclopedia of Nuclear Magnetic Resonance, Vol. 6* (Eds.: D. M. Grant, R. K. Harris), Wiley, New York, **1996**, p. 3988.
[41] T. H. Mourey, S. R. Turner, M. Rubinstein, J. M. J. Fréchet, C. J. Hawker, K. L. Wooley, *Macromolecules* **1992**, *25*, 2401–2406.
[42] M. S. Matos, J. Hofkens, W. Verheijen, F. C. de Schryver, S. Hecht, K. W. Pollak, J. M. J. Fréchet, B. Forier, W. Dehaen, *Macromolecules* **2000**, *33*, 2967–2973.
[43] T. L. Chasse, R. Sachdeva, Q. Li, Z. Li, R. J. Petrie, C. B. Gorman, *J. Am. Chem. Soc.* **2003**, *125*, 8250–8254.
[44] C. B. Gorman, J. S. Smith, *Acc. Chem. Res.* **2001**, *34*, 60–71.
[45] C. B. Gorman, J. C. Smith, M. W. Hager, B. L. Parkhurst, H. Sierzputowska-Gracz, C. A. Haney, *J. Am. Chem. Soc.* **1999**, *121*, 9958–9966.
[46] C. M. Cardona, S. Mendoza, A. E. Kaifer, *Chem. Soc. Rev.* **2000**, *29*, 37–42.
[47] D. Astruc, M.-C. Daniel, J. Ruiz, *Chem. Commun.* **2004**, 2637–2649.
[48] R. Nakajima, M. Tsuruta, M. Higuchi, K. Yamamoto, *J. Am. Chem. Soc.* **2004**, *126*, 1630–1631.

Received: April 11, 2006
Published online: August 3, 2006

